

Charged Higgs Contribution into $t\bar{b}$ -pair Production in Hadronic Collisions

M.V. Foursa¹, D.A. Murashev² and S.R. Slabospitsky³

*State Research Center
Institute for High Energy Physics,
Protvino, Moscow Region 142284
RUSSIA*

Abstract

We investigate the charged Higgs boson contribution into $t\bar{b}$ -pair production in pp -collisions at LHC. It is shown that due to the H^\pm -boson exchange the total yield of $t\bar{b}$ is modified significantly for small and large values of $\tan\beta$. However, for the small values of $\tan\beta$ one should expect also the production of right-handed top quark contrary to pure left-handed t -quark production through W^\pm -boson exchange only. This fact provides a possibility to separate H^\pm and W^\pm contributions by means of the investigations of angular distributions of top decay products. The detailed simulation of the signal and relevant background processes is performed.

Protvino, 2000

¹ fursa@mx.ihep.su

² murashev@mx.ihep.su

³ slabospitsky@mx.ihep.su

1 Introduction

The existence of the charged Higgs boson H^\pm is predicted by many extensions of the Standard Model (see, for example, [1]). The search for a charged Higgs boson is carried out in e^+e^- annihilation at LEP-2 collider at CERN [2] as well as at the Tevatron in the top quark decays [3]. The search for the H^\pm -boson will be one of the main experimental tasks at future LHC machine [4, 5]. The main channels for H^\pm -boson search are the reactions of $gb \rightarrow tH^-$ and $gg \rightarrow t\bar{b}H^-b$ [5, 6, 7].

In the present paper we consider an additional possibility to study a signal from charged Higgs boson in the quark-antiquark annihilation subprocess:

$$q\bar{q}' \rightarrow H^+ \rightarrow t\bar{b}.$$

Namely, we consider the charged Higgs boson contribution to the process of $t\bar{b}$ -pair production in proton-proton collisions

$$pp \rightarrow t\bar{b}X. \tag{1}$$

Note, that $t\bar{b}$ quark production through W -boson exchange in the s -channel had been considered earlier (see [4, 8, 9, 10]). This reaction plays a significant role in the study of electroweak t -quark production. In particular, this process is very important for the investigations of electroweak vertex of tWb interactions [4].

The New Physics beyond the Standard Model (SM) can modify the nature of t -quarks interactions (see [4] and references therein). In particular, the contribution of charged Higgs boson into process (1) can be considered as a manifestation of New Physics. The existence of the H^\pm -boson leads not only to the modification of the total cross section for $t\bar{b}$ -pair production, but also to the change of angular distributions of top quark decay products. The detailed consideration of the contribution due to several forms of the New Physics into $t\bar{b}$ -pair hadronic production as well as the analysis of the top quark polarization properties resulted from such new interactions can be found, for example, in [10].

Here we investigate the charged Higgs boson production in proton-proton collisions at future CERN LHC machine at the energy of $\sqrt{s} = 14$ TeV. Certainly, the strategy for the search for the H^\pm -boson production is determined, in particular, by the Higgs boson mass (see [5]). For relatively light H^\pm , say, $m_{H^\pm} < m_t$, the most promising possibility is the investigation of t -quark decay into H^\pm and b -quark. In the present paper we assume that the charged Higgs is heavier than the top quark. As a result, we consider the top quark decays into $W^\pm b$ pair. Moreover, we consider only leptonic decays of W^\pm -boson, because for hadronic W^\pm decays it is very difficult to separate a signal from a huge QCD background.

Note, that typical differential distributions (p_T and η) of the t -quark and its decay products are practically the same as for the SM production of $t\bar{b}$ -pair (via

W^+ -boson exchange only). Therefore, for the separation of the H^\pm contribution we explore t -quark polarization properties, which are different for $W^+ \rightarrow t\bar{b}$ and $H^+ \rightarrow t\bar{b}$ contributions for small values of $\tan\beta$. We find the specific kinematic cuts, which provide the separation of H^\pm and W^\pm contributions in reaction (1).

The paper is organized as follows. In Section 2 we present an explicit form of matrix elements squared for the considered process. The behavior of the total cross section production of $t\bar{b}$ -pair as a function of m_H and $\tan\beta$ is considered in Section 3. The differential distributions on p_\top and η as well as the angular distributions of top decay products are also discussed in this Section. A detailed simulation of the signal and relevant background processes is given in Section 4. The main results are summarized in the Conclusion.

2 Matrix elements calculations

The Lagrangian describing the $\bar{t}H^\pm b$ -vertex in the two doublet Higgs model has the following form [1, 5, 4]:

$$\mathcal{L} = \sqrt{\frac{G_F}{\sqrt{2}}} H^\pm \{ \tan\beta \bar{U}_L V_{ij} M_D D_R + \cot\beta \bar{U}_R M_U V_{ij} D_L + \tan\beta \bar{N}_L M_L L_R \}, \quad (2)$$

where the symbols U and D refer to 'up' and 'down'-type quarks, while N and L correspond to the charged lepton and neutrino, V_{ij} is the Cabbibo-Kobayashi-Maskawa matrix element, M_D and M_U are the quark masses, and M_L is the mass of charged leptons, $\tan\beta$ is the ratio of values of vacuum expectation value for two Higgs doublets, G_F is the Fermi constant.

The subprocesses of $t\bar{b}$ -pair production through W^\pm and H^\pm exchange,

$$q_1 \bar{q}_2 \rightarrow (H^+ + W^+) \rightarrow t\bar{b}, \quad (3)$$

is described by two diagrams presented in Fig. 1.

The corresponding matrix element squared is presented as a sum of three terms, corresponding to H^\pm -boson (M_H) and W^\pm -boson (M_W) exchanges and their interference (M_I):

$$|M_{2 \rightarrow 2}|^2 = |M_H|^2 + |M_W|^2 + |M_I|^2, \quad (4)$$

where

$$\begin{aligned} |M_H|^2 &= \frac{16G_F^2 |V_{12}|^2 |V_{tb}|^2}{(\hat{s} - m_H^2)^2 + \Gamma_H^2 m_H^2} \left[(m_t^2 \cot^2 \beta + m_b^2 \tan^2 \beta) (p_t p_b) - 2m_b^2 m_t^2 \right] \\ &\quad \times \left[(m_1^2 \cot^2 \beta + m_2^2 \tan^2 \beta) (p_1 p_2) - 2m_1^2 m_2^2 \right], \\ |M_W|^2 &= \frac{128m_W^4 G_F^2 |V_{12}|^2 |V_{tb}|^2}{(\hat{s} - m_W^2)^2 + \Gamma_W^2 m_W^2} (p_t p_2)(p_b p_1), \end{aligned}$$

$$|M_I|^2 = \frac{32G_F^2|V_{12}|^2|V_{tb}|^2m_tm_bA}{A^2+B^2} \times [-m_1^2 \cot^2 \beta(p_tp_2) + m_2^2(p_tp_1) + m_1^2(p_bp_2) - m_2^2 \tan^2 \beta(p_bp_1)],$$

where \hat{s} is the total energy squared of colliding partons, V_{ij} is the Cabbibo-Kobayashi-Maskawa matrix element, Γ_H is the H^+ -boson decay width, m_i and p_i are the quark masses and 4-momenta, respectively, m_W and Γ_W are the W-boson mass and decay width, $A = (\hat{s} - m_W^2)(\hat{s} - m_H^2) + \Gamma_W m_W \Gamma_H m_H$, $B = (\hat{s} - m_W^2)\Gamma_H m_H - (\hat{s} - m_H^2)\Gamma_W m_W$.

Bearing in mind the study of the t -quark polarization properties in reaction (1), we also perform the calculations of subprocesses (3) with the consideration of further top quark decay. Namely, we calculate the matrix element squared for the subprocess $2 \rightarrow 4$:

$$q_1 \bar{q}_2 \rightarrow (H^+ + W^+) \rightarrow \bar{b}t(\rightarrow bW^+) \longrightarrow b\bar{b}l^+\nu_l. \quad (5)$$

Similarly to subprocesses (3), we present the $|M_{2 \rightarrow 4}|^2$ as a sum of three terms corresponding to the H^\pm and the W^\pm exchanges and their interference:

$$|M_{2 \rightarrow 4}|^2 = |M_H|^2 + |M_W|^2 + |M_I|^2, \quad (6)$$

where

$$\begin{aligned} |M_H|^2 &= \frac{2048m_W^4 G_F^4 |V_{tb}|^4 |V_{12}|^2 (p_b k_1)}{((\hat{s} - m_H^2)^2 + \Gamma_H^2 m_H^2) C_W C_t} \\ &\quad \times \{ (q_1, q_2) [m_1^2 \cot^2 \beta + m_2^2 \tan^2 \beta] - 2m_1^2 m_2^2 \} \\ &\quad \times \{ m_b^2 \tan^2 \beta [2(k_2 p_t)(p_{\bar{b}} p_t) - (k_2 p_{\bar{b}}) p_t^2] \\ &\quad + m_t^4 \cot^2 \beta (k_2 p_{\bar{b}}) - 2m_b^2 m_t^2 (k_2 p_t) \}, \\ |M_W|^2 &= \frac{8192m_W^8 G_F^4 |V_{tb}|^4 |V_{12}|^2 (p_b k_1)(p_{\bar{b}}, q_1)}{((\hat{s} - m_W^2)^2 + \Gamma_W^2 m_W^2) C_W C_t} \\ &\quad \times [2(q_2 p_t)(k_2, p_t) - (q_2 k_2) p_t^2], \\ |M_I|^2 &= \frac{4096m_W^6 G_F^4 |V_{tb}|^4 |V_{12}|^2 A m_1 m_2}{(A^2 + B^2) C_W C_t} \\ &\quad \times \{ m_t^2 \cot^2 \beta [(q_1, p_{\bar{b}})(p_t k_2) + (q_1 p_t)(p_{\bar{b}} k_2) - (q_1 k_2)(p_{\bar{b}} p_t)] \\ &\quad + m_t^2 [(q_2 k_2)(p_{\bar{b}} p_t) - (q_2 p_{\bar{b}})(p_t k_2) - (q_2, p_t)(p_{\bar{b}}, k_2)] \\ &\quad + m_b^2 \tan^2 \beta [2(q_2 p_t)(p_t k_2) - (q_2 k_2) p_t^2] \\ &\quad + m_b^2 [(q_1 k_1) p_t^2 - 2(q_1 p_t)(p_t k_2)] \}, \end{aligned}$$

where A and B is defined in (4); $C_W = (p_W^2 - m_W^2)^2 + \Gamma_W^2 m_W^2$ and $C_t = (p_t^2 - m_t^2)^2 + \Gamma_t^2 m_t^2$, p_W and p_t are the momenta of top quark and W -boson, respectively; k_1 and k_2 are the momenta of neutrino and charged lepton.

Note, that the matrix element squared (6) corresponding to subprocess (5) is calculated for the first time.

3 Total cross sections and differential distributions

In our calculations we use the parton distributions from [15]. The evolution parameter Q^2 is chosen to be $Q^2 = \hat{s}$, where \hat{s} is the total energy squared of colliding partons. In our calculations we use the following values of the b and t -quark masses

$$m_b = 4.5 \text{ GeV} \quad [16] \quad \text{and} \quad m_t = 173.8 \text{ GeV}. \quad (7)$$

For the fixed value of the charged Higgs boson mass the largest cross section is expected at large and small values of $\tan\beta$. The behavior of the cross section for reaction (1) as a function of the H^\pm -boson mass and $\tan\beta$ is presented in Fig. 2. Note, that the cross section reaches its maximum at $m_H \sim 200$ GeV due to the pole character of cross section under consideration (see (4)).

The H^\pm -boson contribution into reaction (1) leads to the increasing of the $t\bar{b}$ -pair cross section production. However, the modification of the “observable” number of events, $N_{ev}(Wb\bar{b}) \sim \sigma(t\bar{b}) \times B(t \rightarrow bW^+)$, depend on m_{H^\pm} . For the H^\pm -boson lighter than top quark ($m_{H^\pm} < m_t$), the branching fraction of $t \rightarrow bW$ decay ($B(t \rightarrow bW)$) may significantly decrease [5, 4]. As a result, we should expect the decrease of N_{ev} as compared to the SM case. For heavy H^\pm -boson ($m_{H^\pm} > m_t$) there is no $t \rightarrow bH^+$ decay channel. Therefore, one has $B(t \rightarrow bW^+) \approx 1$ and we should expect the increase of $W^+ b\bar{b}$ yield.

The “experimentally seen” cross sections for t -quark production in the reaction (1), i.e.

$$\sigma(pp \rightarrow \bar{b}t(\rightarrow bW)X) = \sigma(pp \rightarrow t\bar{b}X) \times B(t \rightarrow bW) \quad (8)$$

are presented in Fig. 3 for two values of $m_H=90$ and 200 GeV. Note, that for the small and large values of $\tan\beta$ the H^\pm -boson contribution leads to a noticeable modification of the $t\bar{b}$ -pair production, while for an intermediate range of $\tan\beta = 0.8 \div 20$ the H^\pm contribution becomes negligible. The differential distributions of the final particles (t, W, b, l) on transverse momentum and pseudorapidity calculated at the parton level are shown in Figs. 4, 5. As is shown in the figures, the differential distributions for the cases of H^+ and W^+ exchange have practically the same shapes. Therefore, the contribution of New Physics may lead only to the deviation of the expected number of events. Therefore, to elucidate the nature of possible deviation from the SM predictions, one needs to examine additional quantities which have a differential behavior for the SM and beyond SM cases.

For this purpose we explore the polarization properties of the t -quark, widely considered in the literature (see, for example, [4, 11, 12] and references therein). It is well known that subprocess (3) leads to the production of almost left-handed t -quark [4, 10]. At the same time the charged Higgs boson contribution leads to the

production of right(left)-handed t -quark for small (large) values of $\tan\beta$ (see [5]). Note, that for the left-handed t -quark the b -quark (the charged lepton) should fly mostly alongside (opposite) to the direction of the top quark momentum (see [4, 10]). Naturally, for the right-handed quark one has the reverse situation.

Hereafter, in order to separate the W^\pm and H^\pm contributions, we examine the angular distributions,

$$\frac{dN}{d\cos\theta^*}, \quad (9)$$

where θ^* is the angle in the top rest frame between the direction of the top quark momentum and the momentum of the final particle from the top quark decay $t \rightarrow b\nu$.

In Fig. 6 we present the corresponding angular distributions of the b -quark and charged lepton from t -quark decay calculated by means of the matrix element (6) separately for only W^+ or H^\pm exchange (see the histograms “a, b, e, f” in the Fig. 6). For evaluating these distributions, we set $m_{H^\pm} = 200$ GeV and $\tan\beta = 0.1$.

4 Signal and background calculations

We perform the detailed simulation of process (1) with the subsequent top quark decays into electron and muon ($t \rightarrow b e \nu_e$ and $t \rightarrow b \mu \nu_\mu$) and relevant background reactions for the three-year low luminosity run of LHC

$$\sqrt{s} = 14 \text{ TeV} \quad \text{and} \quad \int \mathcal{L} dt = 30 \text{ fb}^{-1}. \quad (10)$$

As an example we choose the values of the charged Higgs boson parameters as follows:

$$m_{H^\pm} = 200 \text{ GeV} \quad \text{and} \quad \tan\beta = 0.1. \quad (11)$$

Note, that our result is not very sensitive to the m_H value, however, the chosen small value of $\tan\beta$, namely, $\tan\beta < 0.2$, is important for further analysis.

For the simulation of the signal and background processes we use the **TOPREX 2.51** event generator [19]. At present the TOPREX provides the generation at the parton level, the production of $t\bar{t}$ -pair, three processes of single top (“ Wg ”, “ tW ”, and “ W^* ”) and $Wb\bar{b}$ production with subsequent top quark decay into bW and W into fermion anti-fermion pair. One can generate also several processes of top quark production via anomalous t -quark interactions [20].

We use the PYTHIA 6.134 [17] for simulation of quarks and gluons hadronization. We perform the simulation with taking into account the ability of CMS detector at LHC [14]. For “fast” detector simulation all the events are passed through the package CMSJET 4.703 [18]. As a result, the final event contains the information about momenta of “detected” photons, charged leptons (e, μ), hadronic jets and missing energy E_{mis} (see [18] for details). The efficiencies for b -tagging of jets

originating from b -quark, c -quark and light partons (u, d, s -quarks and gluon) are about 60%, 10%, and $1 \div 2\%$, respectively [18]. In what follows we refer to the b -tagged jet as the B -jet.

For our choice of the H^\pm -boson parameters, (see (11)), the cross section for $(t\bar{b} + \bar{t}b)$ production in reaction (1) due to H^\pm -boson contribution at $\sqrt{s} = 14$ TeV is equal to

$$\sigma(H^\pm) = 9.7 \text{ pb.} \quad (12)$$

There are several sources of the background to the considered process (1). We present here the cross section values of these processes evaluated at LO approximation. The consideration of the higher order corrections is given, for example, in [4]. These background processes are as follows (all the cross section values imply the summation on particles and anti-particles):

- three processes of single top production

$$\begin{aligned} q\bar{q}' &\rightarrow W^\pm \rightarrow t\bar{b}, & \sigma(W^*) &= 7.5 \text{ pb}, \\ gq &\rightarrow q't\bar{b}, & \sigma(Wg) &= 180 \text{ pb}, \\ gb &\rightarrow tW, & \sigma(tW) &= 60 \text{ pb} \end{aligned}$$

- $t\bar{t}$ -pair production: $gg(q\bar{q}) \rightarrow t\bar{t}, \quad \sigma(t\bar{t}) = 600 \text{ pb}$
- $W b\bar{b}$ production: $q\bar{q}' \rightarrow W b\bar{b}, \quad \sigma(Wb\bar{b}) = 360 \text{ pb}$
- $W + jets$ production (generated by PYTHIA)

$$\sigma(W + jets) = 59000 \text{ pb}$$

Signal process (1) and all the background reactions (except $W+jets$) are simulated by using TOPREX generator. For evaluation of the last process ($W+jets$) the PYTHIA parameter k_{Tmin} is chosen to be equal to 2 GeV (i.e. CKIN(1)=2 [17]).

Process (1) of $t\bar{b}$ pair production with the subsequent top decay into $b\nu$ is characterized by the presence in the final state of one charged isolated lepton (from W -boson decay), the missing energy (neutrino) and two hard B -jets from b -quarks.

The appropriate cuts providing a signal selection from the background processes, are considered in detail in [4]. In particular, these cuts include the requirement of two “hard” B -jets:

$$\text{“hard”-cut : } p_T(B_1, B_2) \geq p_{T0} \sim 75 \text{ GeV} \quad (13)$$

However, this cut leads to an essential modification of the form of the corresponding $\cos\vartheta^*$ distributions (9) of the top quark decay products.

Indeed, in Fig. 6 we present the angular distributions of the b -quark (from t -quark decay) evaluated at the parton level before and after the cut on the b -quark

transverse momentum (see the histograms “b, c, f, g” in Fig. 6). One can see that after application of the cut (13) the form of the angular distribution of b -quark, originating from the decay of right-handed t -quark (produced via H^\pm exchange) changes dramatically and even becomes qualitatively similar to that of b -quark from left-handed top decay (produced via W^\pm exchange). In view of actual possibilities of the detector it will be even more difficult to distinguish these two distributions.

Therefore, we propose another p_T -cut (“soft-hard”) on the final B -jets. Namely, we require that p_T of one B_1 -jet (from top quark) should not exceed some value of $p_{T1} = 100$ GeV, while p_T of the other B_2 -jet should be greater than $p_{T0} = 75$ GeV:

$$\text{“soft – hard” – cut : } p_T(B_1 \text{ from } t) \leq p_{T1} \text{ and } p_T(B_2) \geq p_{T0}. \quad (14)$$

It is seen from the histograms “d” and “h” in Fig. 6 that this “soft-hard” cut (14) saves the forms of angular distributions of the decay products of t -quarks, produced through H^\pm and W^\pm exchange.

In the further analysis we apply both variants (13) and (14) of p_T cuts. Thus, for signal/background separation we require

- 1) one and only one isolated lepton (with $p_T > 10$ GeV) and at least two hadronic jets (with $p_T > 20$ GeV and pseudorapidity $|\eta| < 4.5$),
- 2) explicitly two b -tagged jets (with $p_T > 25$ GeV and $|\eta| < 2.5$) and no other hadronic jets,
- 3) the transverse momentum of the reconstructed W -boson and two B_1 and B_2 jets should not exceed of 10 GeV, $|\vec{p}_T(W B_1 B_2)| \leq 10$ GeV,
- 4) H (“hard”)-cut on p_T of B -jets ($p_T(B_1, B_2) \geq 75$ GeV),
- 4') SH (“soft-hard”)-cut on p_T of B -jets (one B_1 -jet with $p_T \leq 100$ GeV and second B_2 -jet with $p_T \geq 75$ GeV),
- 5) the reconstructed mass of the t -quark should be within $150 \div 200$ GeV, $|M_{rec}(BW) - m_t| < 25$ GeV.

As usual, using the four-momentum of charged lepton and the transverse momentum of missing energy for the reconstruction of W -boson momentum, we get two solutions for $p_{rec}(W)$. For further reconstruction of top quark four-momentum, $p_{rec}(t)$, we should examine both two B -jets for the case of H -cut (13). As a result, we obtain four combinations for the reconstructed momentum of the t -quark. For SH -cut (14) we assume that the B_1 -jet with the smallest transverse momentum results from the t -quark decay and we have two solutions for $p_{rec}(t)$. Then, the invariant mass of the $(W B)$ -system, $M(WB)$, with the value nearest to $m_t = 173.8$ GeV is

treated as a reconstructed value of the t -quark mass. The corresponding $p_{rec}(t)$ is considered as a reconstructed t -quark momentum.

The resulted efficiencies after application of all the cuts to the signal and the background are given in Table 1. One can see that new SH cut (14) provides slightly better efficiency for the signal reconstruction. However, the background suppression becomes also worth as compared to the application of old H -cut (13). The resulted number of reconstructed events (for $\int \mathcal{L} dt = 30 \text{ fb}^{-1}$) and the corresponding signal-to-background ratios are given in Table 2. It is seen that the application of the old and new p_T -cuts result in almost the same S/B ratios. Therefore, both of the two variants of p_T -cut (SH and H) provide a rather well reconstruction of the top quark in reaction (1).

The distributions on the reconstructed top quark mass are presented in Fig. 7. The symbol “SM” corresponds to calculations with the SM case, while the symbol “SM+ H^\pm ” corresponds to the SM and H^\pm -boson contribution. The standard fit gives the following values of the reconstructed t -quark mass (in GeV):

	SM	SM + H^\pm
S-H	172.4 ± 11.8	171.6 ± 11.4
H	172.8 ± 11.2	172.4 ± 10.8

Now we proceed to the separation of the H^\pm -boson contribution into reaction (1). For this purpose we explore the difference in $\cos \vartheta_l^*$ -distributions resulted from different polarizations of the t -quark, produced within the SM (only W exchange) and within $W^\pm + H^\pm$ exchange (see Fig. 6). The distributions on $\cos \vartheta_l^*$, calculated for the sum of the signal and background events are given in Fig. 9. The upper two histograms correspond to new SH -cut, while two lower histograms are obtained by application of old H -cut. We fit these distributions by linear dependence on $\cos \vartheta_l^*$:

$$\frac{dN}{d \cos \theta_l^*} \propto 1 + \alpha \cdot \cos \theta_l^* \quad (15)$$

The results of the fit are given in Table 3. It is evident that the new SH -cut (14) is more sensitive to H^\pm -boson contribution. Indeed, the presence of charged Higgs leads to change of the sign of the slope of $\cos \vartheta_l^*$ -distribution, while the application of the old H -cut leads only to modification of the slope α (see Table 3).

Certainly, this result depends on the relative value of the H^\pm -boson contribution. Indeed, for a larger value of the $\tan \beta$ we should expect the decreasing of charged Higgs contribution and, as a result, the values of α should be more close to SM expectations. Note, that for the large value of $\tan \beta > 10$, where we have a noticeable charged Higgs contribution, the produced top quark should be left-handed. As a result, the angular distribution should be the same as in the SM case.

5 Conclusion

In the present paper the contribution from charged Higgs bosons into the process of electroweak production of $t\bar{b}$ -pair at LHC is considered and analyzed in detail. The expressions for matrix elements squared for the corresponding subprocesses are obtained and the role of the t -quark polarization is investigated. The cross sections and angular distributions at a parton level are calculated. The simulation of the signal and relevant background processes by means of PYTHIA in view of opportunities of the CMS detector at LHC is also performed.

We show that the differential distributions (p_T and η) of the t -quark and its decay products are practically the same as for the SM production of $t\bar{b}$ -pair. As a result, by using a conventional way for the top quark separation from the background, it would be difficult to distinguish the H^\pm -boson from W^\pm -boson exchange. At the same time the produced top quark through charged Higgs exchange has different polarization in comparison to the SM case. At small values of $\tan\beta$, one should expect the production of the right-handed t -quarks. The corresponding angular distributions of leptons essentially differ from those predicted by the SM.

In order to separate the W^\pm and H^\pm contributions into reaction (1) we propose the new p_T -cut (14) for b -tagged hadronic jets. This “soft-hard” p_T -cut provides not only the t -quark signal discrimination from the background processes, but also the selection of the contribution to the relevant process from a charged Higgs boson.

Certainly, the proposed p_T -cut can help only for the small values of $\tan\beta < 0.2$. For the larger values (i.e., for $\tan\beta > 0.2$) one needs find other variables, which should be sensitive to charge Higgs boson contribution into reaction (1). In principle, we can explore the SM prediction for the difference in top and anti-top quark production cross sections in reaction (1). This difference results due to the absence of the valence anti-quark contributions in the proton-proton collisions [9, 13]. At the same time, the main contribution to the $H^\pm \rightarrow t\bar{b}$ process comes from the interaction of charmed and strange quarks from initial hadrons. Since in the pp -collisions we have equal numbers of the c , s quarks and anti-quarks, we should expect $\sigma(H^+ \rightarrow t\bar{b}) \approx \sigma(H^- \rightarrow \bar{t}b)$. Thus, the study of asymmetry in t - and \bar{t} -quarks production in reaction (1) may provide an additional possibility to separate the charged Higgs boson contribution.

Acknowledgment

We are thankful to E. Boos, D. Denegri, V. Drollinger, V. Ilyin, A. Kostritsky, N. Krasnikov, M. Mangano, A. Nikitenko, V. Obraztsov, L. Sonnenschein, N. Stepanov and T. Tait for fruitful discussions. The work of S.R.S. was supported, in part, by Russian Foundation for Basic Research, projects no. 99-02-16558.

References

- [1] J.F. Gunion, H.E. Haber, G.L. Kane, and S. Dawson, “The Higgs Hunters’ Guide” (Addison-Wesley, Reading, MA, 1990).
- [2] R. Barate *et al.* [ALEPH Collaboration], CERN-EP-2000-086 [hep-ex/0008005];
P. Abreu *et al.* [DELPHI Collaboration], Phys. Lett. **B460** (1999) 484;
M. Acciarri *et al.* [L3 Collaboration], Phys. Lett. **B466** (1999) 71 [hep-ex/9909044];
K. Ackerstaff *et al.* [OPAL Collaboration], Phys. Lett. **B426** (1998) 180 [hep-ex/9802004].
- [3] T. Affolder *et al.* [CDF Collaboration], Phys. Rev. **D62** (2000) 012004 [hep-ex/9912013];
B. Abbott *et al.* [D0 Collaboration], Phys. Rev. Lett. **82** (1999) 4975 [hep-ex/9902028].
- [4] M. Beneke *et al.*, “Top quark physics,” hep-ph/0003033.
- [5] A. Djouadi *et al.*, “The Higgs working group: Summary report,” hep-ph/0002258.
- [6] A.C. Bawa, C.S. Kim, and A.D. Martin, Z. Phys. **C47** (1990) 75;
V. Barger, R.J.N. Phillips, and D.P. Roy, Phys. Lett. **B324** (1994) 236;
S. Moretti and K. Odagiri, Phys. Rev. **D55** (1997) 5627;
J.F. Gunion, Phys. Lett. **B322** (1994) 125;
F. Borzumati, J.-L. Kneur, and N. Polonsky, Phys. Rev. **D60** (1999) 115011;
D. J. Miller, S. Moretti, D. P. Roy and W. J. Stirling, Phys. Rev. **D61** (2000) 055011 [hep-ph/9906230].
- [7] R. Kinnunen, J. Tuominiemi, and D. Denegri, *Search for the charged Higgs boson from top decays in CMS*, CMS TN/94-233 (1994).
- [8] S. Cortese and R. Petronzio, Phys. Lett. **B253**, (1991) 494;
T. Stelzer and S. Willenbrock, Phys. Lett. **B357**, 125 (1995) [hep-ph/9505433].
- [9] A. P. Heinson, A. S. Belyaev and E. E. Boos, Phys. Rev. **D56** (1997) 3114 [hep-ph/9612424];
A.S. Belyaev, E.E. Boos and L.V. Dudko, Phys. Rev. **D59**, 075001 (1999) [hep-ph/9806332].
- [10] T. Tait and C.-P. Yuan, hep-ph/9710372;
T. M. Tait, hep-ph/9907462;
T. Tait and C.-P. Yuan, hep-ph/0007298.

- [11] M. Jezabek and J. H. Kühn, Nucl. Phys. **B320**, 20 (1989);
M. Jezabek, “Top quark physics,” Nucl. Phys. Proc. Suppl. **37B**, 197 (1994)
hep-ph/9406411.
- [12] G. Mahlon and S. Parke, Phys. Rev. **D55**, 7249 (1997) hep-ph/9611367;
G. Mahlon and S. Parke, Phys. Lett. **B476**, 323 (2000) [hep-ph/9912458];
E. L. Berger and T. M. Tait, hep-ph/0002305;
C. A. Nelson and L. J. Adler, hep-ph/0007086.
- [13] G. V. Jikia and S. R. Slabospitsky, Phys. Lett. **B295** (1992) 136.
- [14] CMS Technical Proposal, CERN/LHC/94-43 LHCC/P1 (1994).
- [15] H. L. Lai *et al.* [CTEQ Collaboration], Eur. Phys. J. **C12** (2000) 375 [hep-ph/9903282].
- [16] *Review of particle physics*, D.E. Groom *et al.*, Eur. Phys. J. **C15** (2000) 1.
- [17] T. Sjöstrand and M. Bengtsson, Comput. Phys. Comm. **43** (1987) 367;
T. Sjöstrand, *PYTHIA 5.7*, Comput. Phys. Comm. **82** (1994) 74.
- [18] S. Abdullin, A. Khanov and N. Stepanov, *CMSJET*, CMS TN/94-180 (1999).
- [19] S.R. Slabospitsky *et al.*, CMS Technical Note, in preparation.
- [20] Y. P. Gouz and S. R. Slabospitsky, Phys. Lett. **B457** (1999) 177 [hep-ph/9811330].

Table 1: The efficiencies (in %) of the signal (H^\pm) and background separation after application of cuts. The symbols SH and H correspond to the usage of new (14) and old (13) p_T -cut.

	H^\pm	W^\pm	Wg	Wt	$t\bar{t}$	Wbb	$W+\text{jets}$
SH	0.77	0.5	0.012	0.008	0.003	0.02	$5 \cdot 10^{-5}$
H	0.26	0.4	0.007	0.003	0.003	0.01	–

Table 2: The number of events resulted after application of all the cuts. In the calculations the total integrated luminosity of $\int \mathcal{L} dt = 30 \text{ fb}^{-1}$ is assumed. The symbols W/B and H/B correspond to signal-to-background ratios, calculated within the SM framework as well as for the SM and H^\pm -boson contribution, respectively. The symbol SH(H) stands for the usage of new (old) p_T -cut.

	H^\pm	W^\pm	SM	SM + H^\pm	$\frac{W}{B}$	$\frac{H}{B}$
SH	470	260	960	1430	0.37	0.49
H	260	220	610	870	0.55	0.43

Table 3: The result of the fit of $\frac{dN}{d \cos \theta_l^*}$ distribution by the function of $(1 + \alpha \cdot \cos \theta_l^*)$. The symbol “SM” corresponds to the calculations with the SM case, while the symbol “SM+ H^\pm ” corresponds to the SM and H^\pm -boson contribution.

	$\alpha(\text{SM})$	$\alpha(\text{SM} + H^\pm)$
SH	-0.29 ± 0.06	$+0.21 \pm 0.05$
H	-0.98 ± 0.05	-0.46 ± 0.06

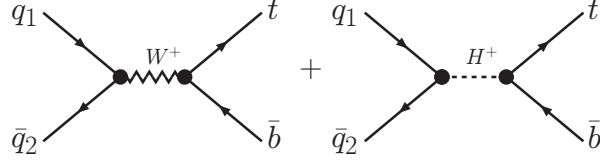


Figure 1: Feynman diagrams for the subprocess $q_1 \bar{q}_2 \rightarrow (W^\pm H^\pm) t \bar{b}$

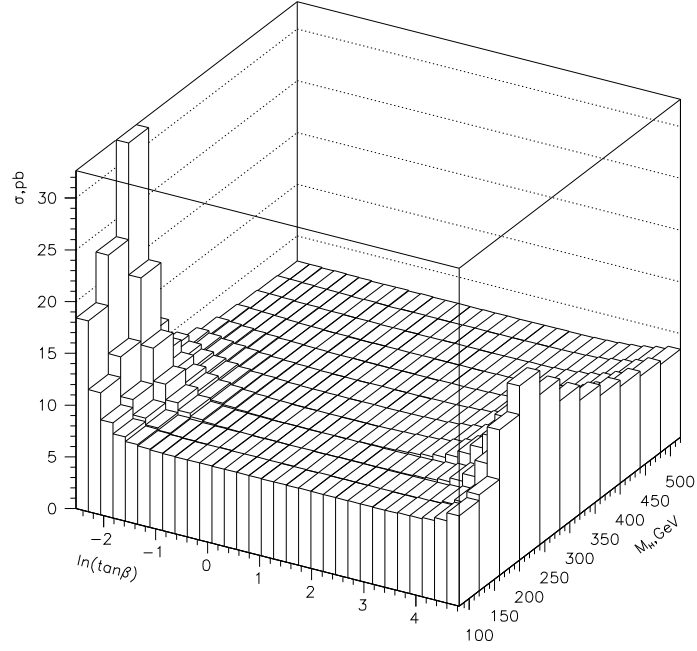


Figure 2: The behavior of the total cross section for $(t\bar{b} + \bar{t}b)$ -pair production in pp -collision at $\sqrt{s} = 14$ TeV as a function of $\tan \beta$ and charged Higgs mass m_H .

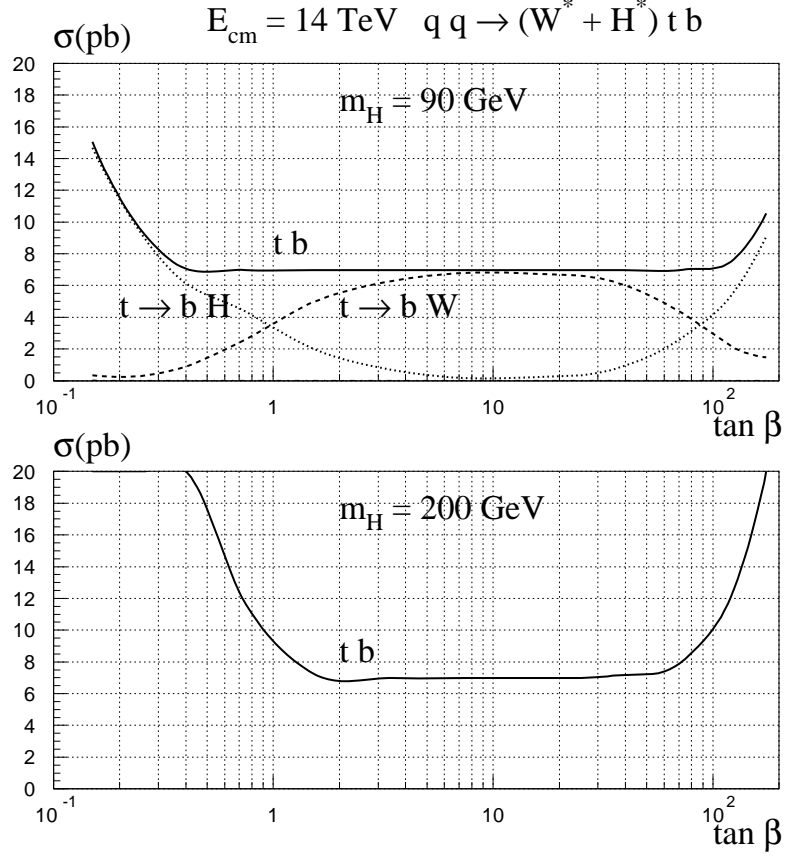


Figure 3: The dependence of the $(t\bar{b} + \bar{t}b)$ -pair production cross section versus $\tan \beta$ for two values of $m_H = 90$ and 200 GeV (the solid curves). The dashed and dotted curves correspond to the cross section production times the branching ratio of t -quark decays into bW^\pm and bH^\pm , respectively.

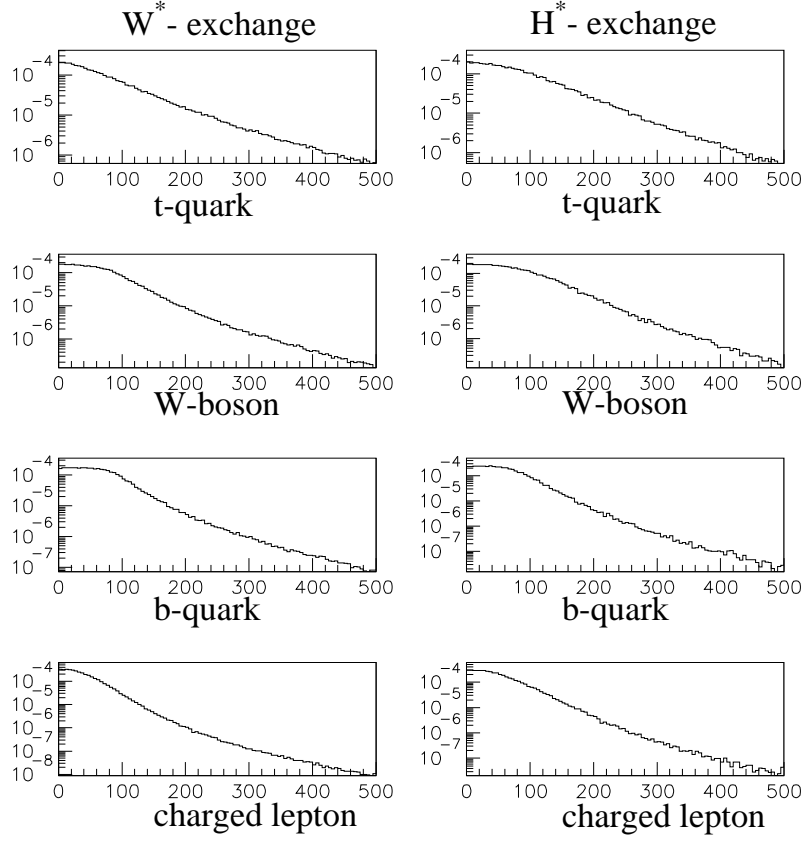


Figure 4: The p_T -distribution of the top quark and the products of its decay $t \rightarrow bW(\rightarrow bl\nu)$ produced in reaction (1). The $\frac{d\sigma}{dp_T}$ is in arbitrary units, while p_T (the x -axis) is in GeV. The symbol W^* (H^*) corresponds to $t\bar{b}$ -pair production through W^\pm (H^\pm)-exchange only.

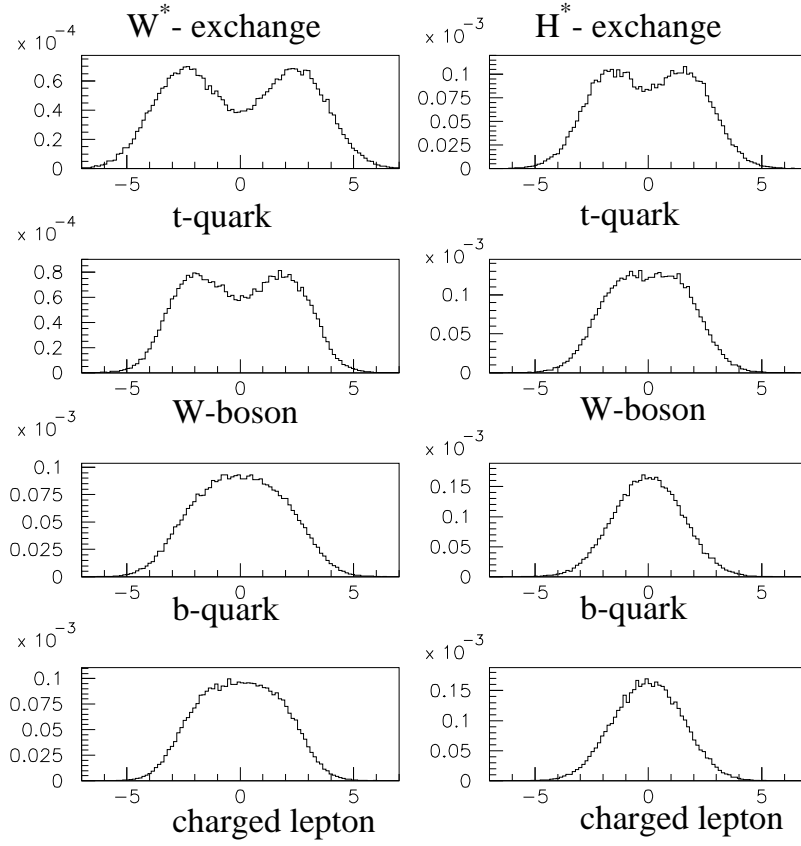


Figure 5: The pseudorapidity, η , distributions of the t -quark and its decay products. For additional explanation see Fig.4.

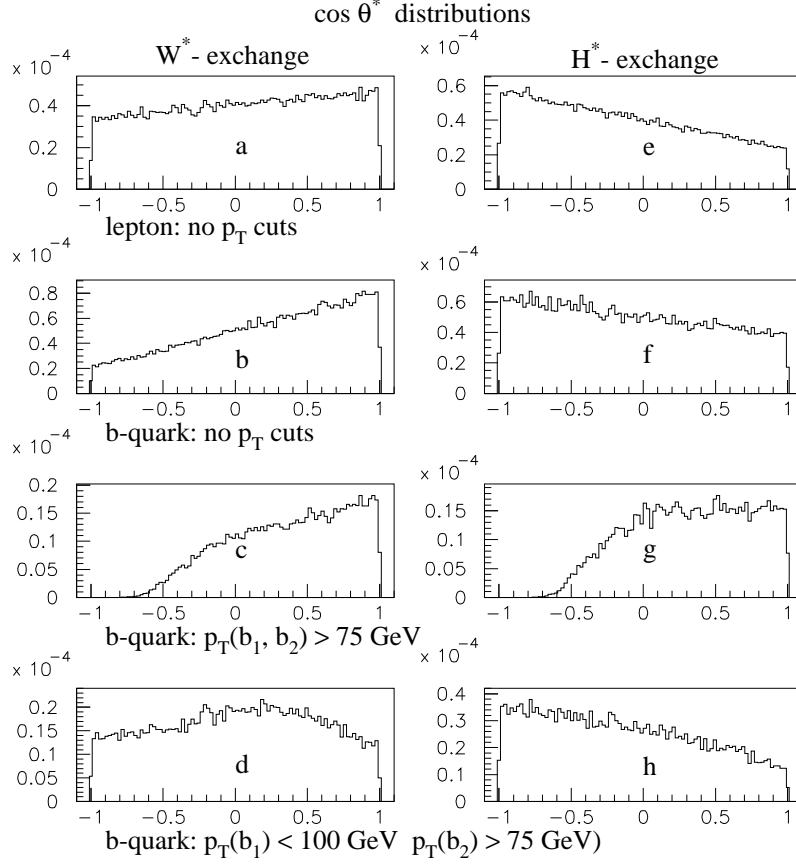


Figure 6: The $\cos \vartheta^*$ -distributions of the charged lepton and b -quark originating from the t -quark decay. All the distributions are obtained from the evaluation of reaction (1) at the parton level for W^\pm -boson exchange (W^*) and H^\pm -boson contribution (H^*). The histograms “a, b, e, f” are obtained without any cuts. The H-cut (13) and SH-cut (14) are used for production of “c, g” and “d, h” histograms, respectively.

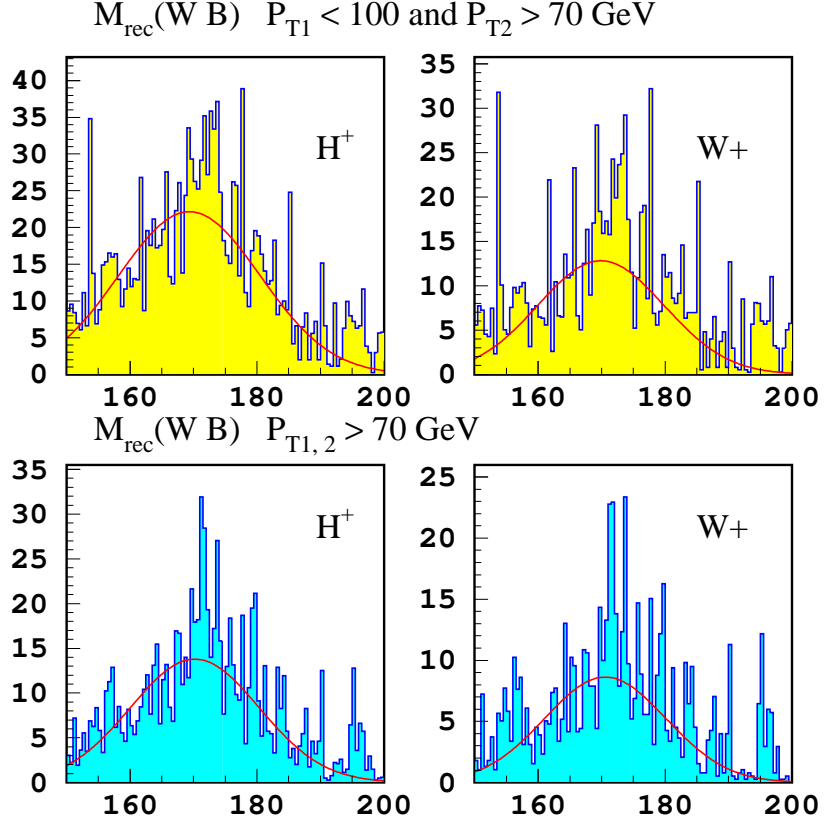


Figure 7: The distributions (in the arbitrary units) on the invariant mass of the $(W B)$ -system, M_{rec} (in GeV) resulted after application of all 1–5 cuts. Two upper and lower histograms correspond to the application of the new SH-cut (14) and old H-cut (13), respectively. The symbol W^+ corresponds to the SM and background processes, while the symbol H^+ refers to the H^\pm , the SM and background contributions.

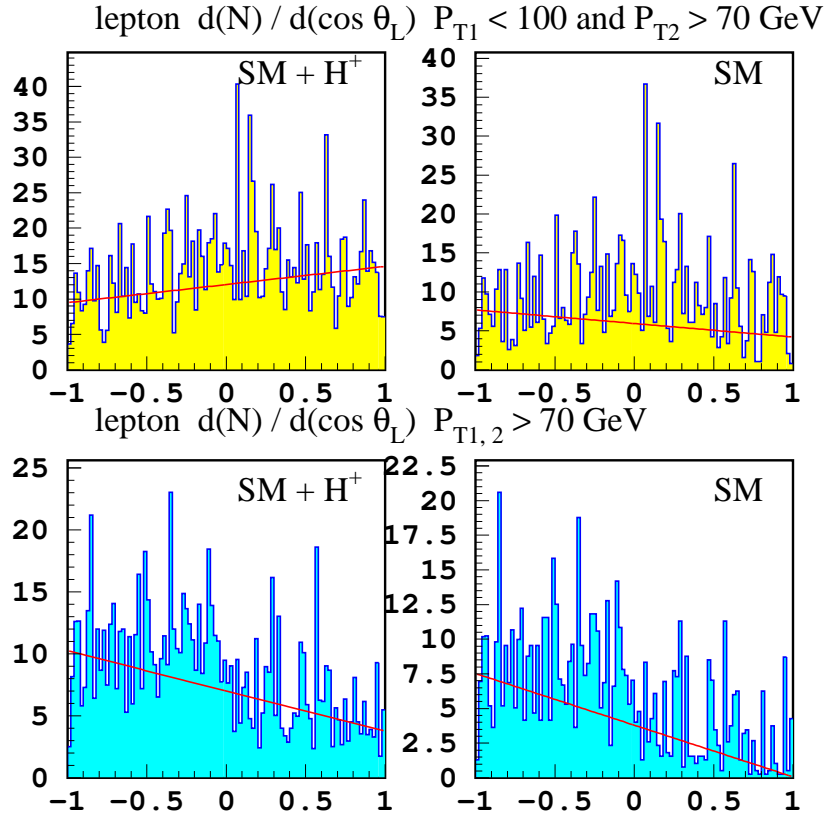


Figure 8: The $\cos \vartheta^*$ -distributions for the charged lepton. The lines correspond to the fit to linear dependence of (15).